ChemBioChem

Supporting Information

Shedding Light on the D_1-Like Receptors: A Fluorescence-Based Toolbox for Visualization of the D_1 and D_5 Receptors

Niklas Rosier, Denise Mönnich, Martin Nagl, Hannes Schihada, Alexei Sirbu, Nergis Konar, Irene Reyes-Resina, Gemma Navarro, Rafael Franco, Peter Kolb, Paolo Annibale, and Steffen Pockes*

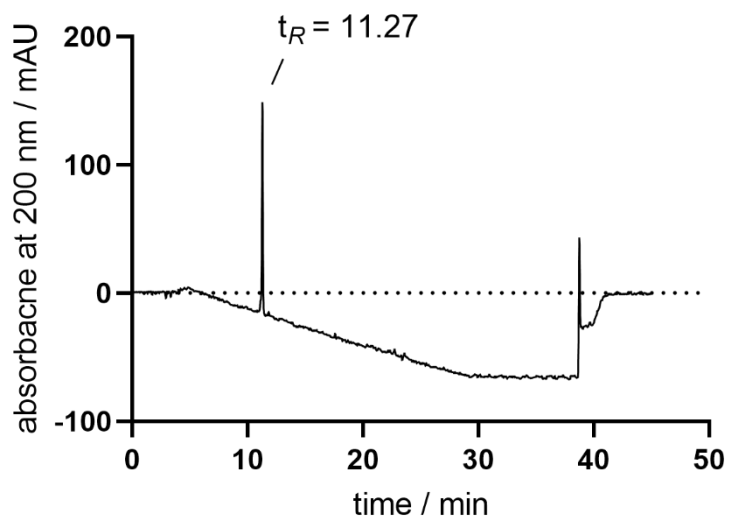**Contents**

1. Chemical purity and stability

Figure S1. RP-HPLC analysis (purity control) of **23** (> 97 %, 220 nm).
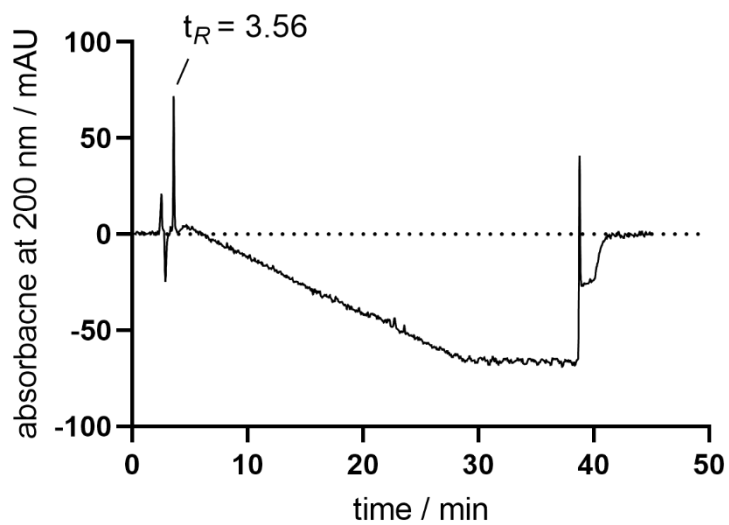

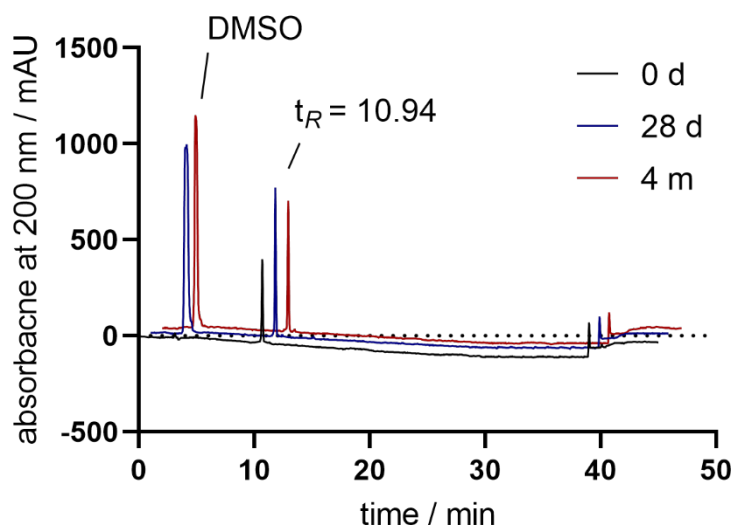**Figure S2.** RP-HPLC analysis (purity control) of **24** (> 97 %, 220 nm).

Figure S3. RP-HPLC analysis (purity and stability control) of **25** (> 98 %, 220 nm). Stability at -18 °C after 28 days and 4 months.
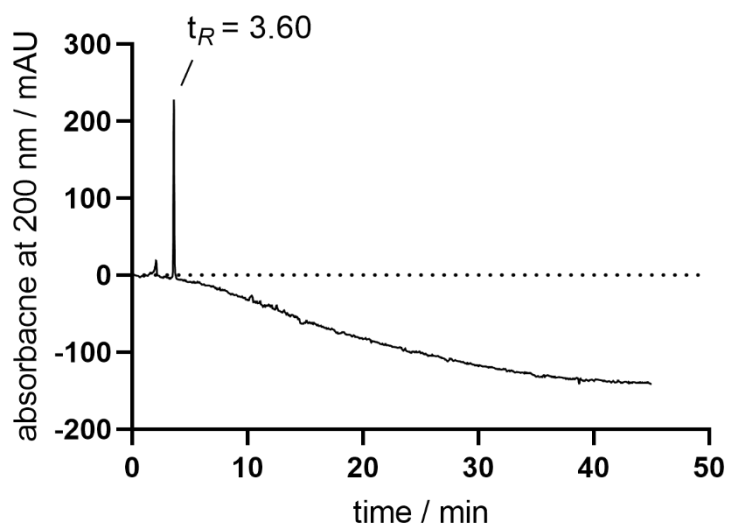

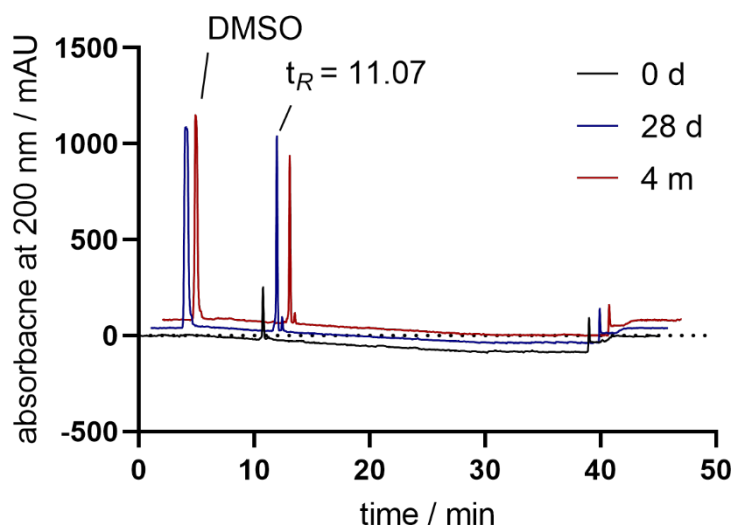**Figure S4.** RP-HPLC analysis (purity control) of **26** (> 96 %, 220 nm).

Figure S5. RP-HPLC analysis (purity and stability control) of **27** (> 95 %, 220 nm). Stability at -18 °C after 28 days and 4 months.
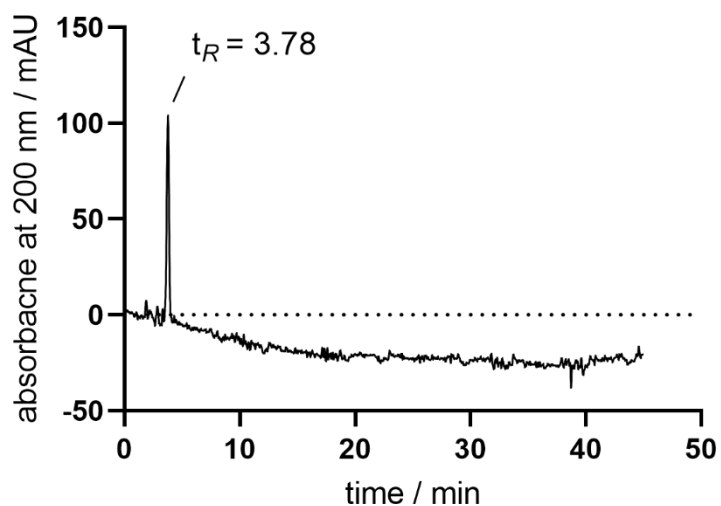

Figure S6. RP-HPLC analysis (purity control) of **28** (> 95 %, 220 nm).
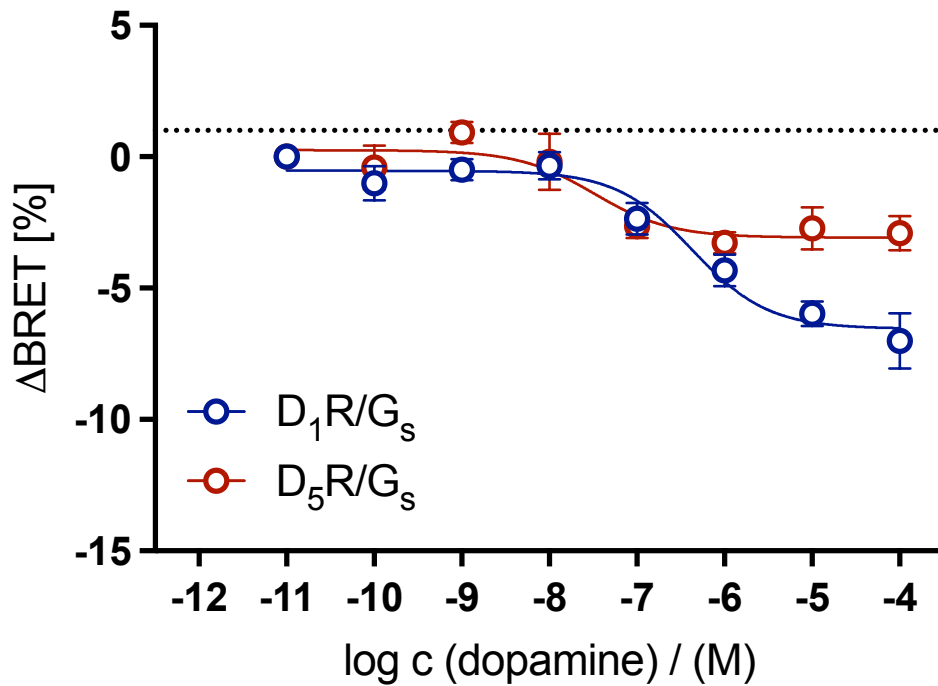
2. Dopamine-induced G_s activation

Figure S7. Concentration−response curves (CRCs) for G_s activation of dopamine in HEK293A cells transiently expressing the G_s BRET sensor along with the wild-type D_1R or D_5R. Graphs represent the means of five (D_1R) or four (D_5R) independent experiments each performed in duplicate. Data were analyzed by nonlinear regression and were best fitted to sigmoidal concentration-response curves.
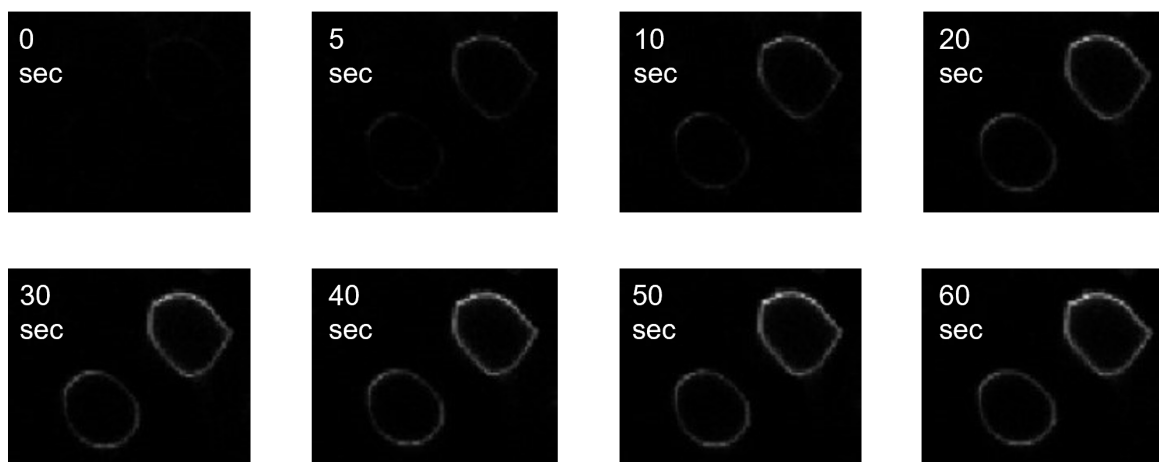
3. Confocal microscopy

Figure S8. Association of **25** to the hD_1R at HEK-293T cells using LSCM. Time-lapse confocal microscopy images of **25** (c = 50 nM) at HEK-293T cells transiently expressing the hD_1R (**A**).
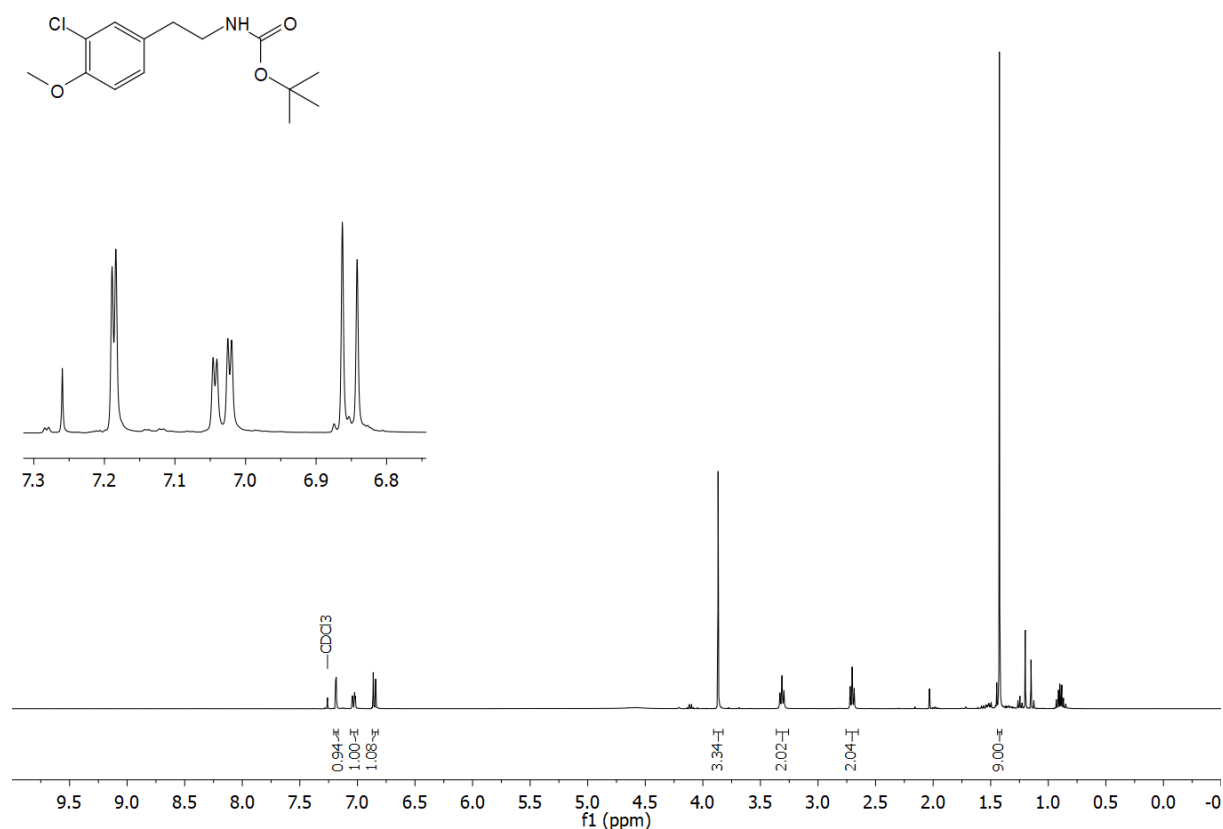
4. NMR spectra
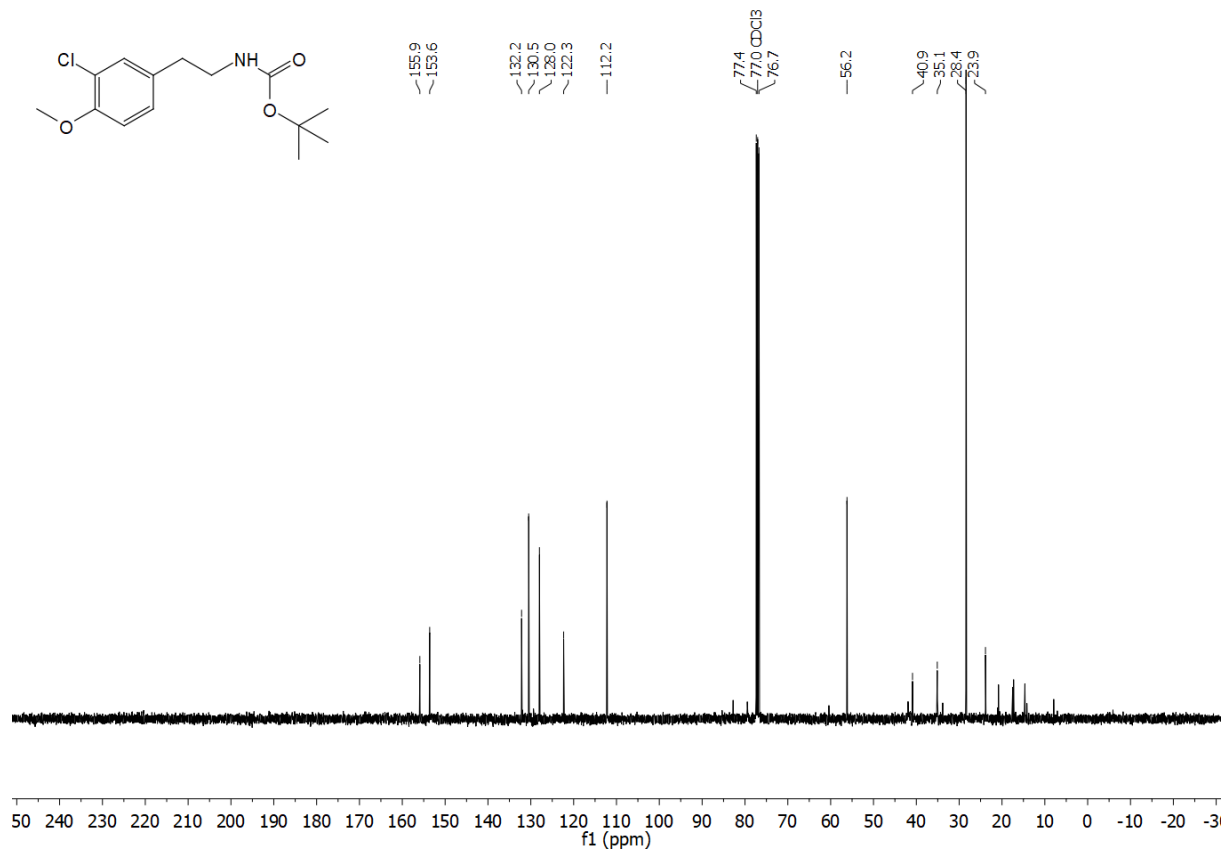

Figure S9. ^{1}H NMR spectrum (400 MHz, CDCl$_3$) of compound **7**.

Figure S10. ^{13}C NMR spectrum (101 MHz, CDCl$_3$) of compound **7**.

Figure S11. ^{1}H NMR spectrum (300 MHz, CDCl$_3$) of compound **10**.

Figure S12. ^{13}C NMR spectrum (75 MHz, CDCl$_3$) of compound **10**.

Figure S13. ^{1}H NMR spectrum (300 MHz, CDCl$_3$) of compound **12a**.
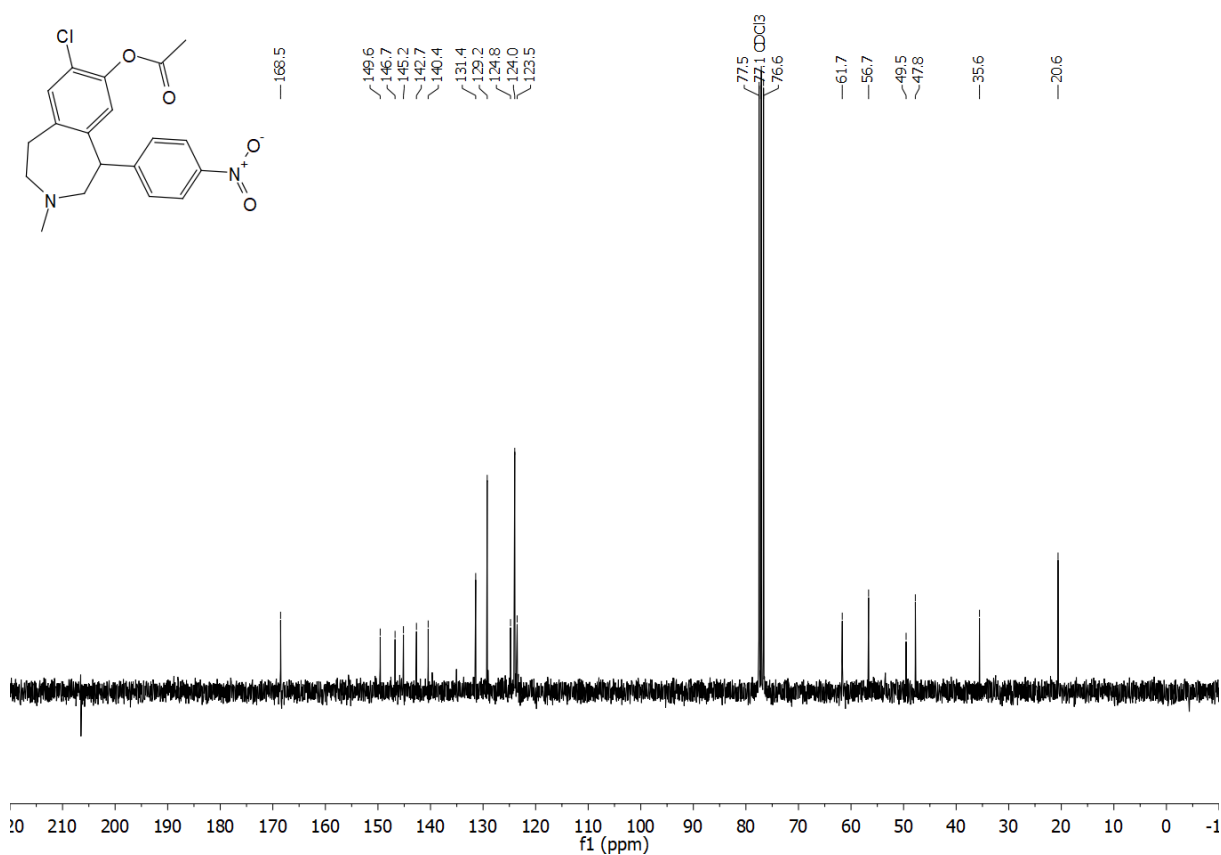

Figure S14. ^{13}C NMR spectrum (75 MHz, CDCl$_3$) of compound **12a**.
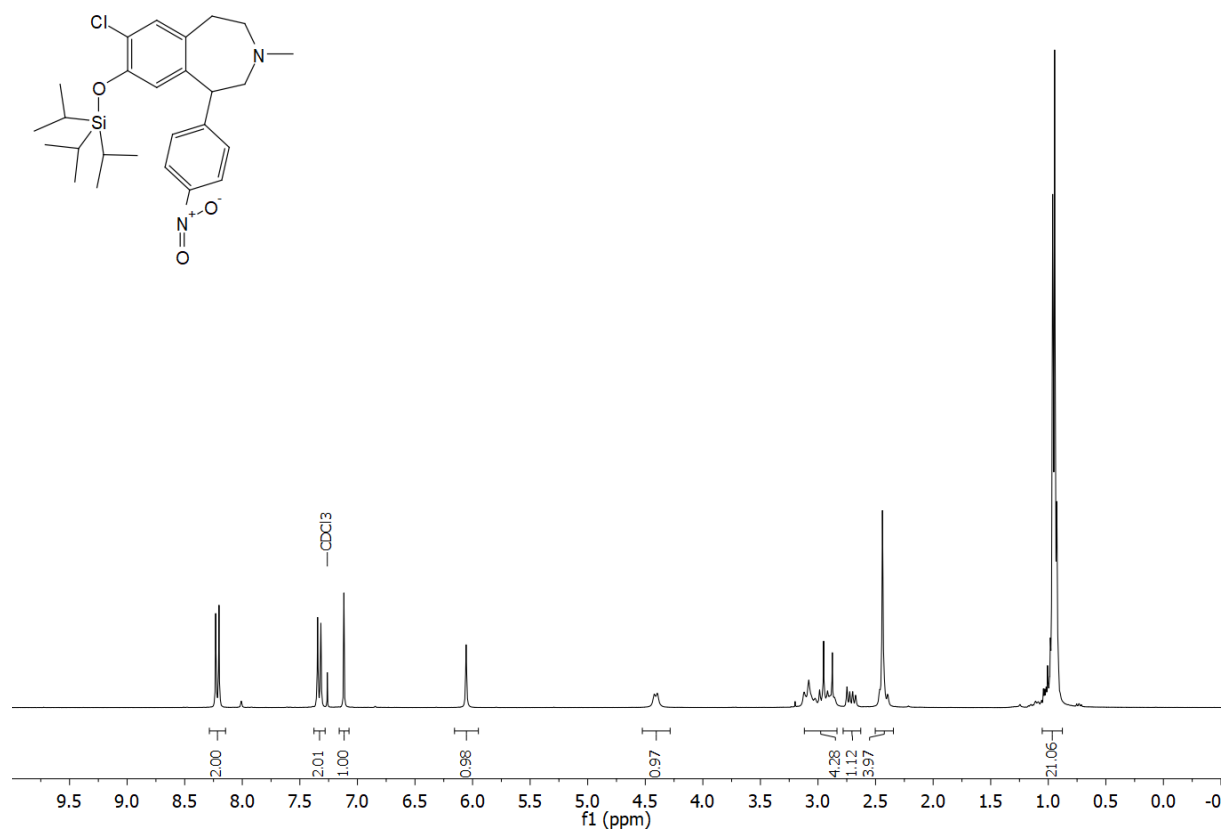
Figure S15. ^{1}H NMR spectrum (300 MHz, CDCl$_3$) of compound **12b**.
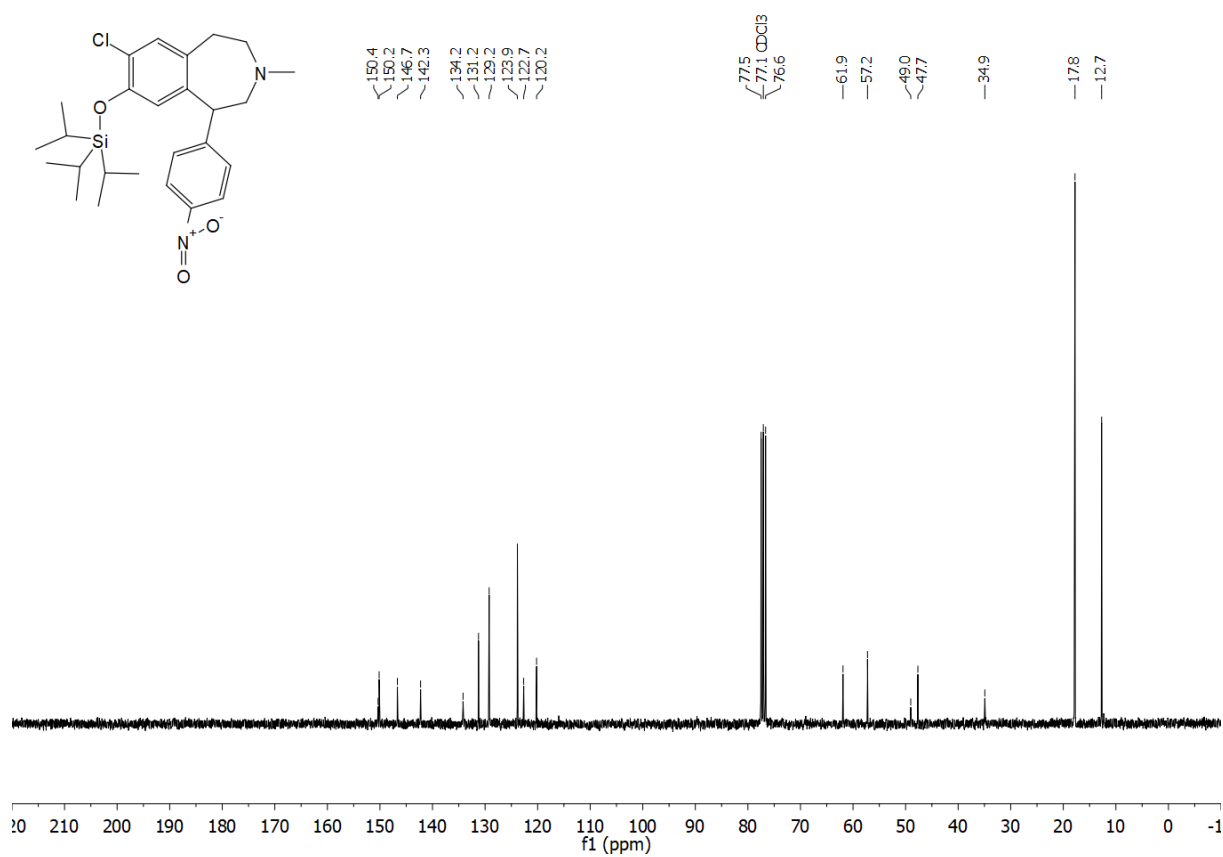

Figure S16. ^{13}C NMR spectrum (75 MHz, CDCl$_3$) of compound **12b**.
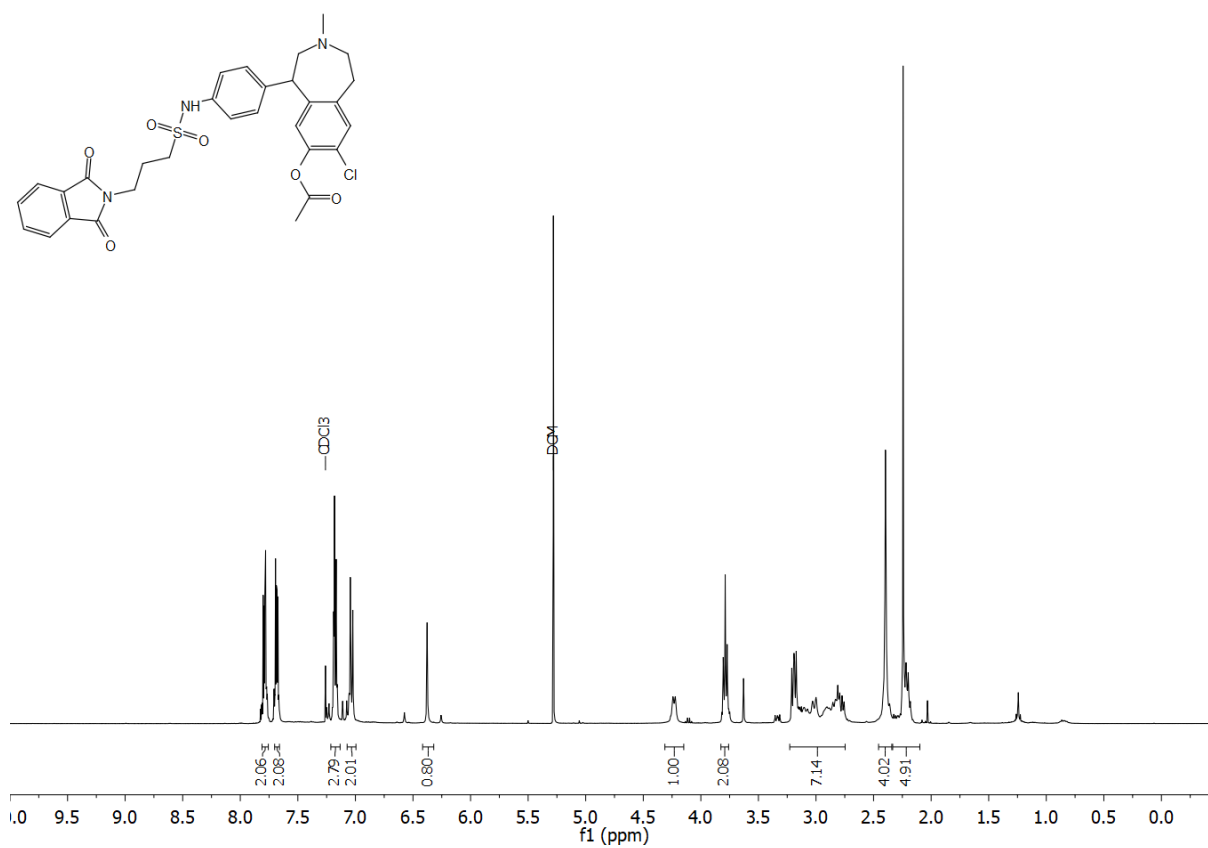
Figure S17. ^{1}H NMR spectrum (400 MHz, CDCl$_3$) of compound **18**.
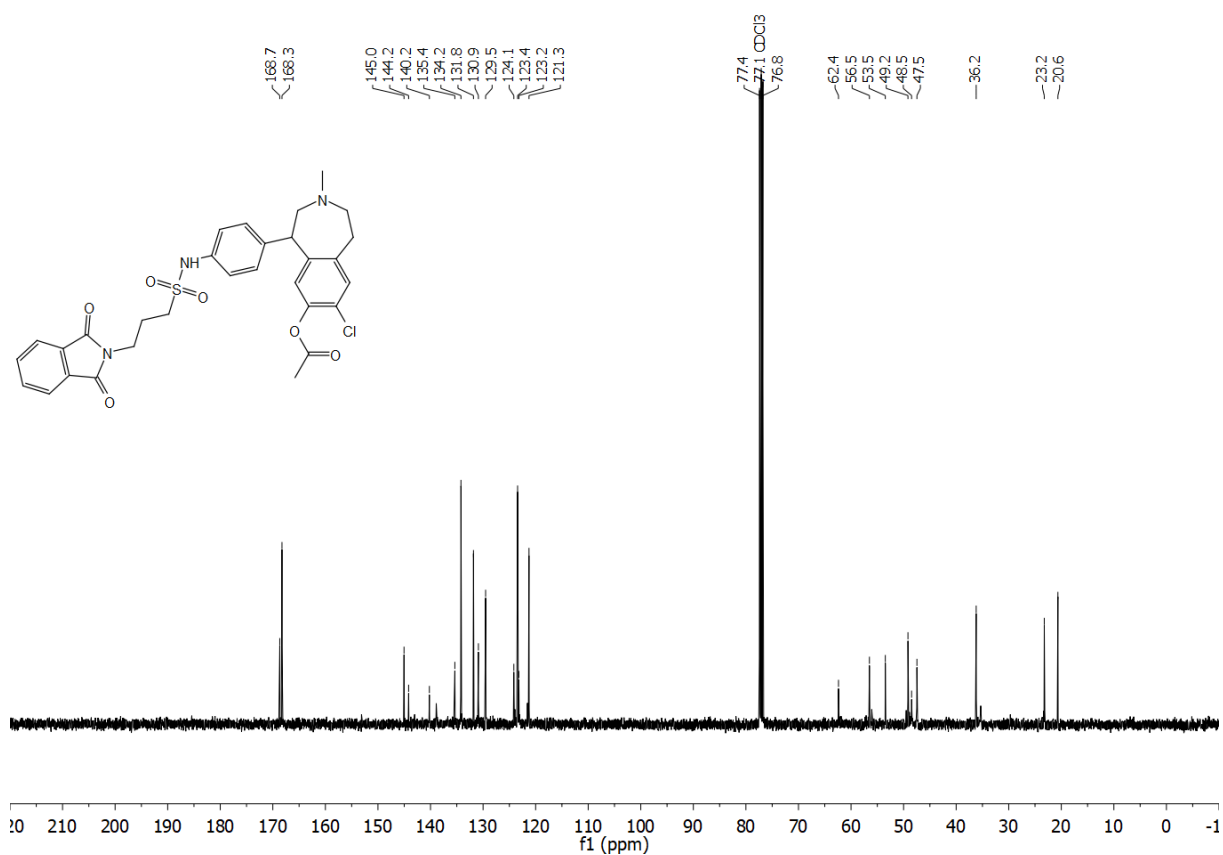

Figure S18. ^{13}C NMR spectrum (101 MHz, CDCl$_3$) of compound **18**.
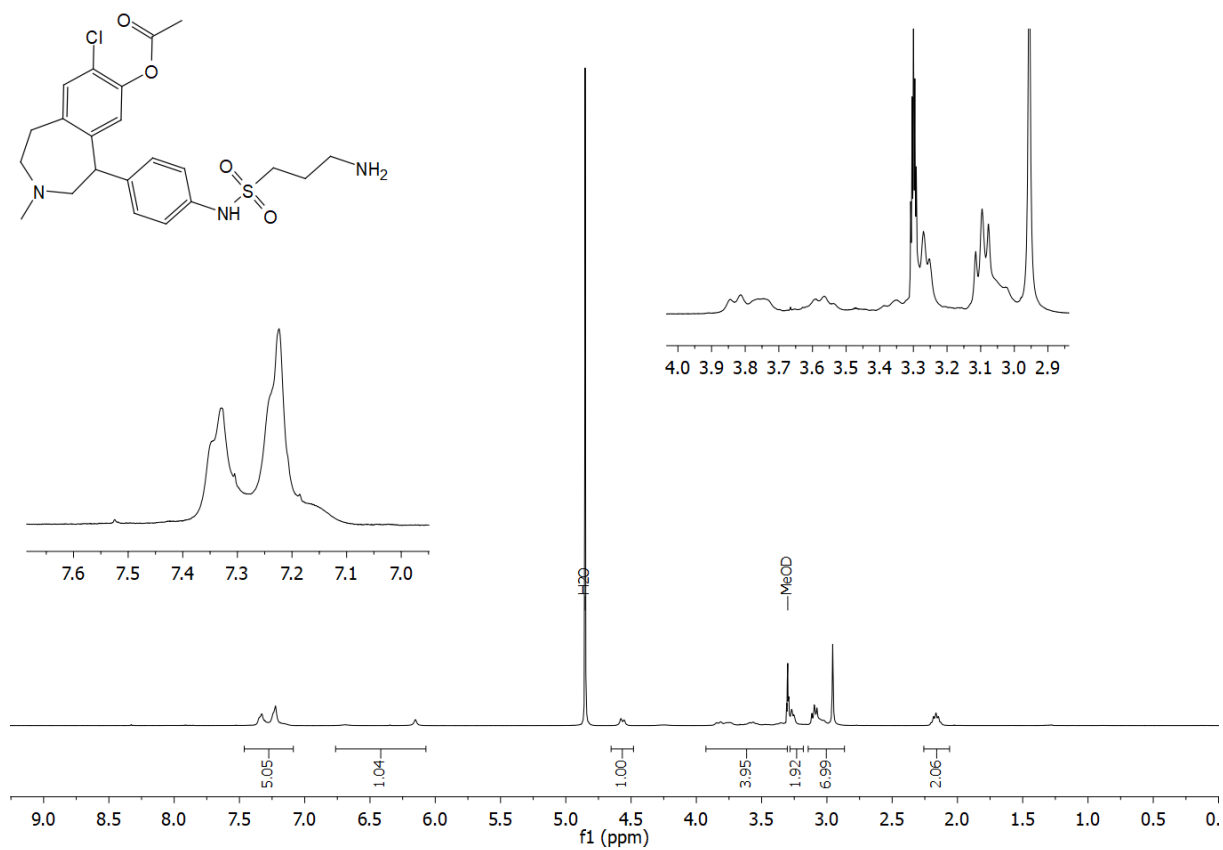
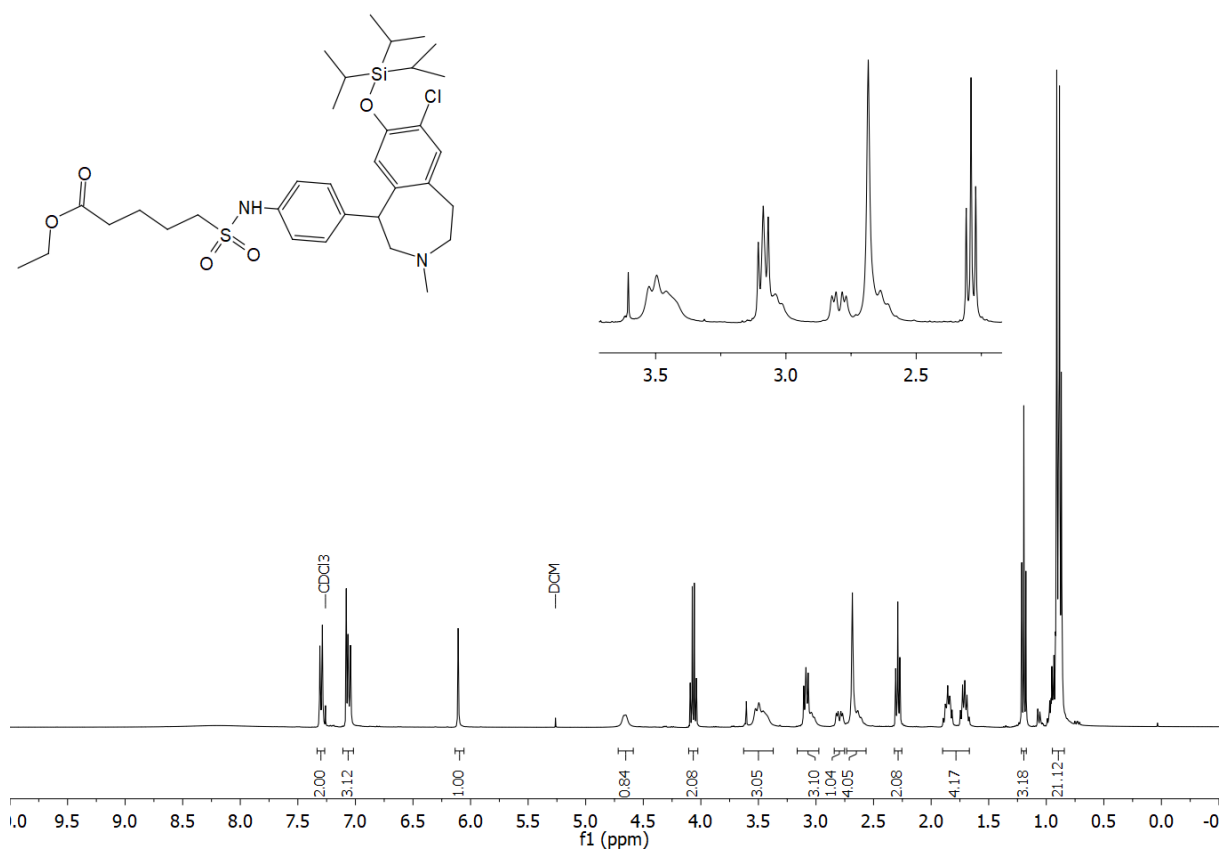**Figure S19.** ^{1}H NMR spectrum (400 MHz, MeOD) of compound **19**.

Figure S20. ^{1}H NMR spectrum (400 MHz, CDCl$_3$) of compound **20**.

Figure S21. ^{13}C NMR spectrum (101 MHz, CDCl$_3$) of compound **20**.

Figure S22. ^{1}H NMR spectrum (400 MHz, MeOD) of compound **21**.

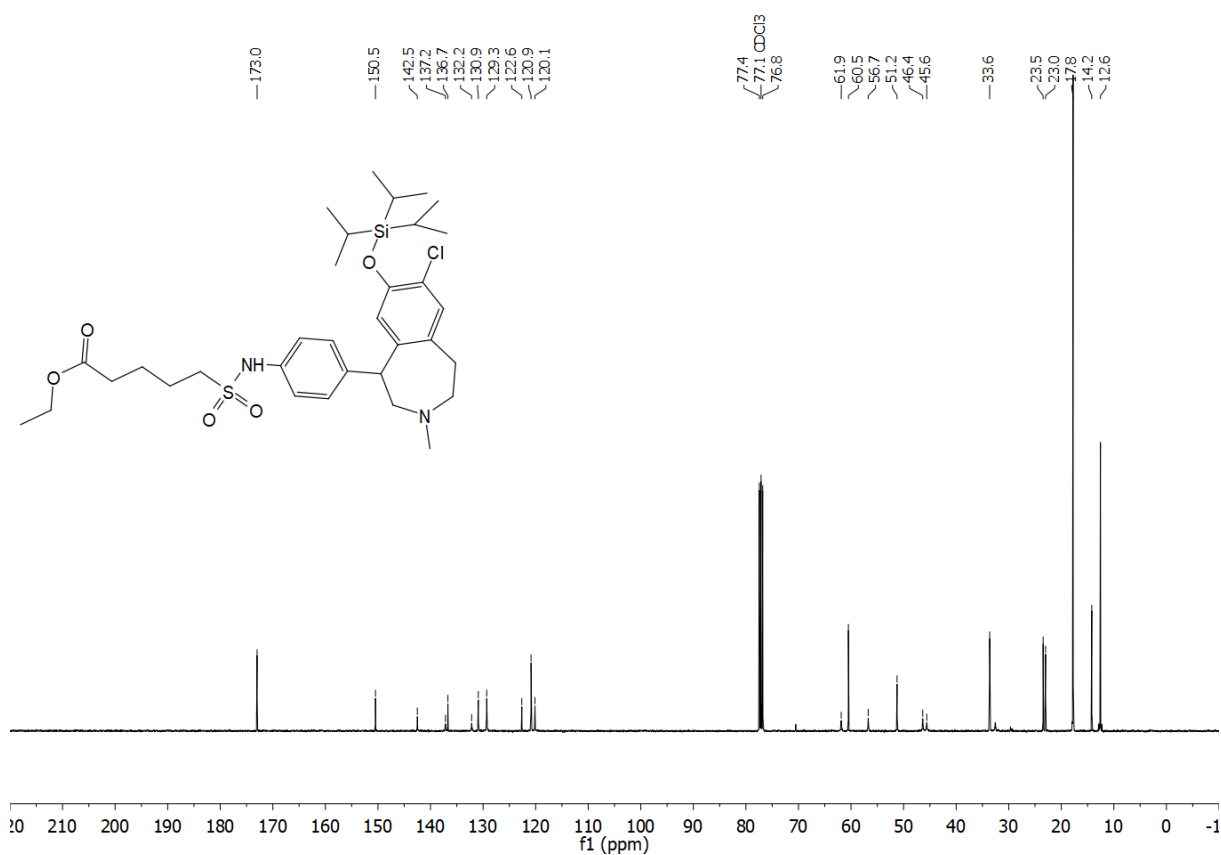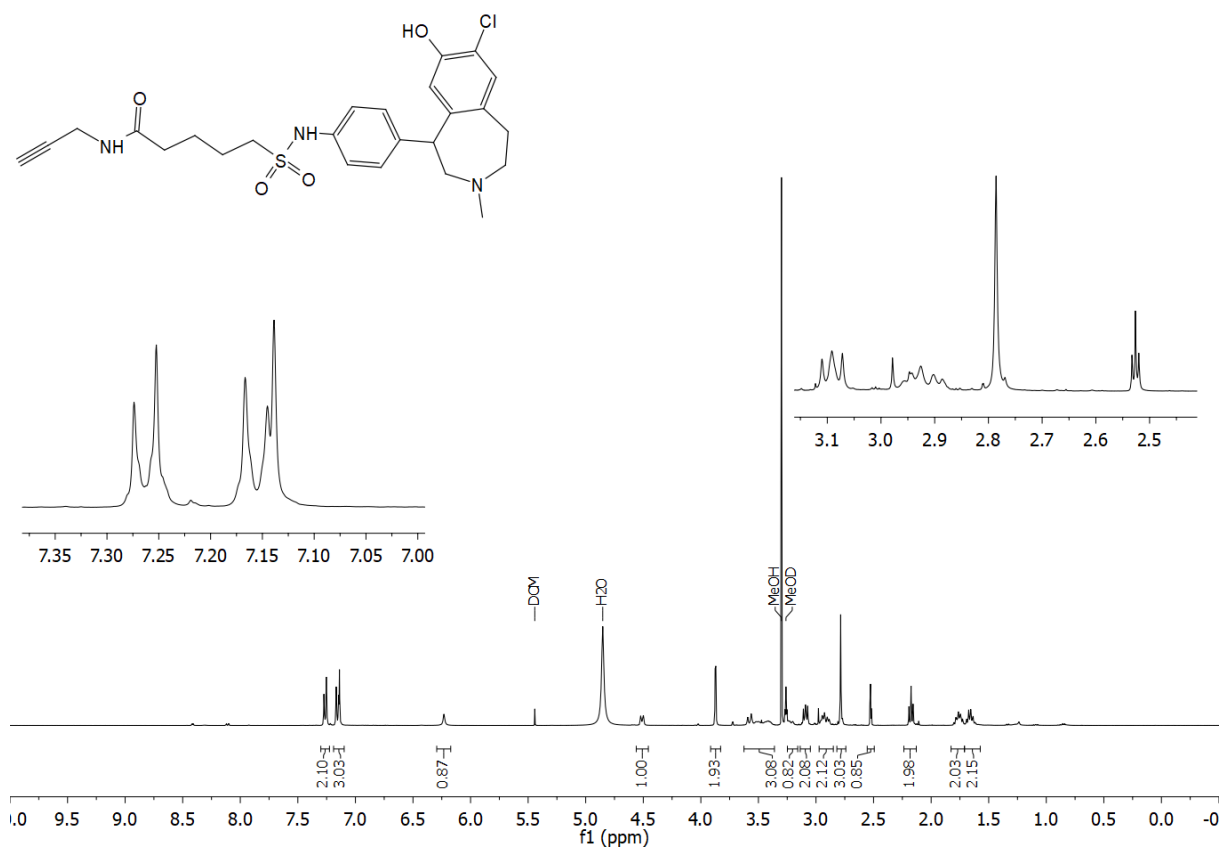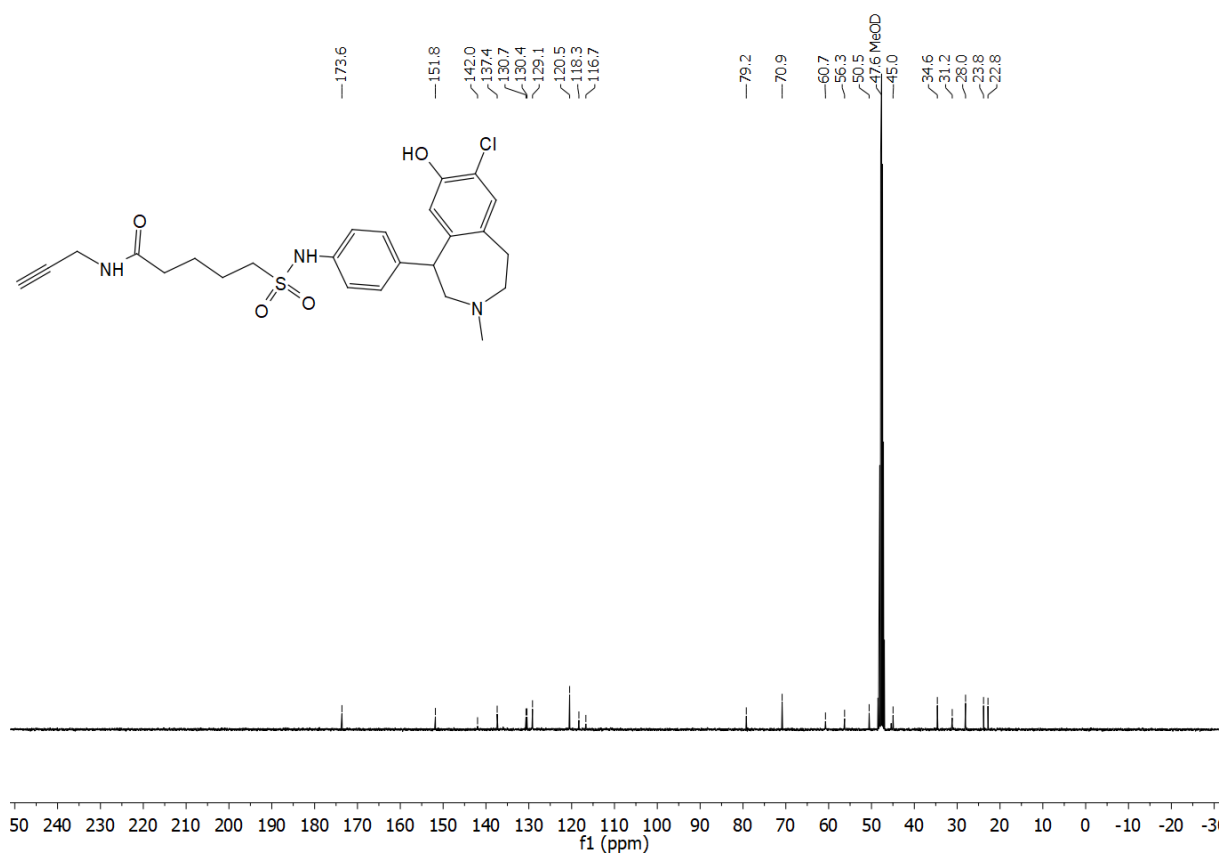**Figure S23.** ^{13}C NMR spectrum (101 MHz, MeOD) of compound **21**.
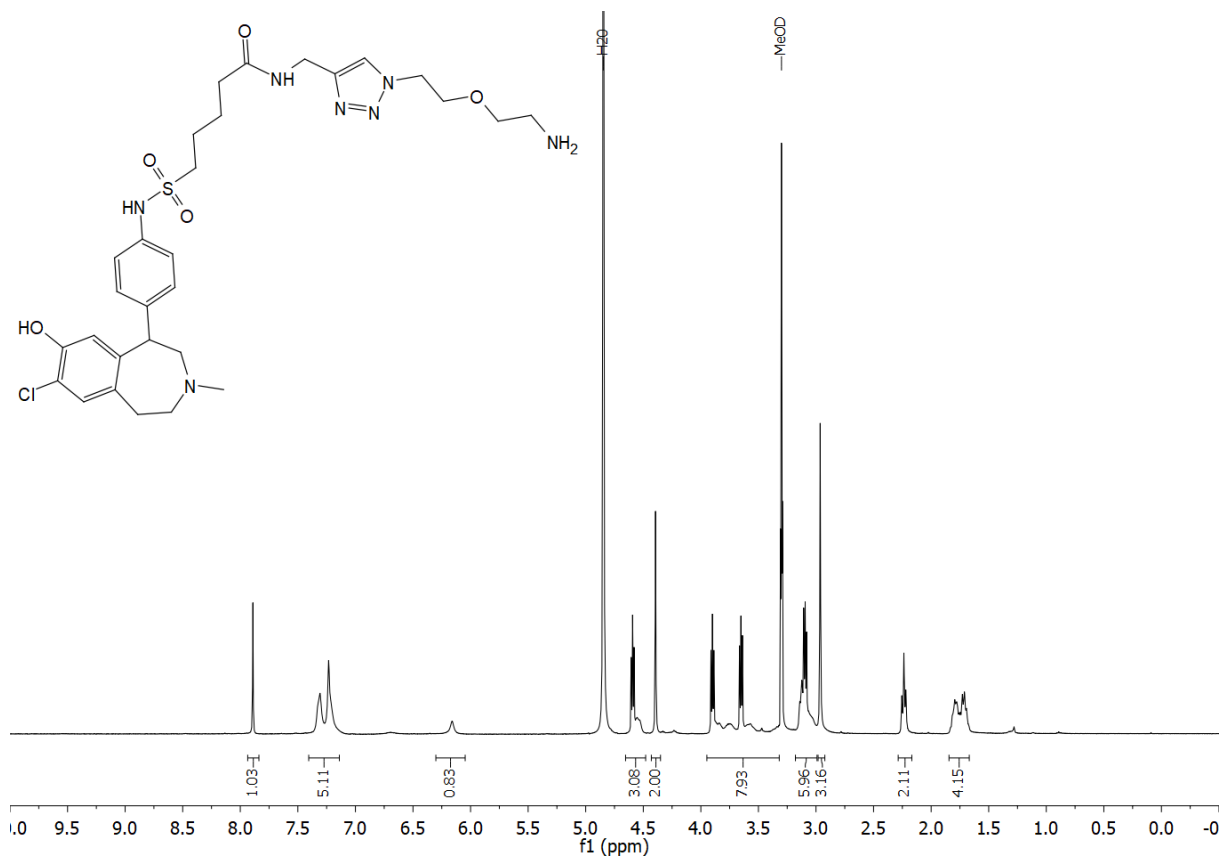
Figure S24. ¹H NMR spectrum (400 MHz, MeOD) of compound **22a**.

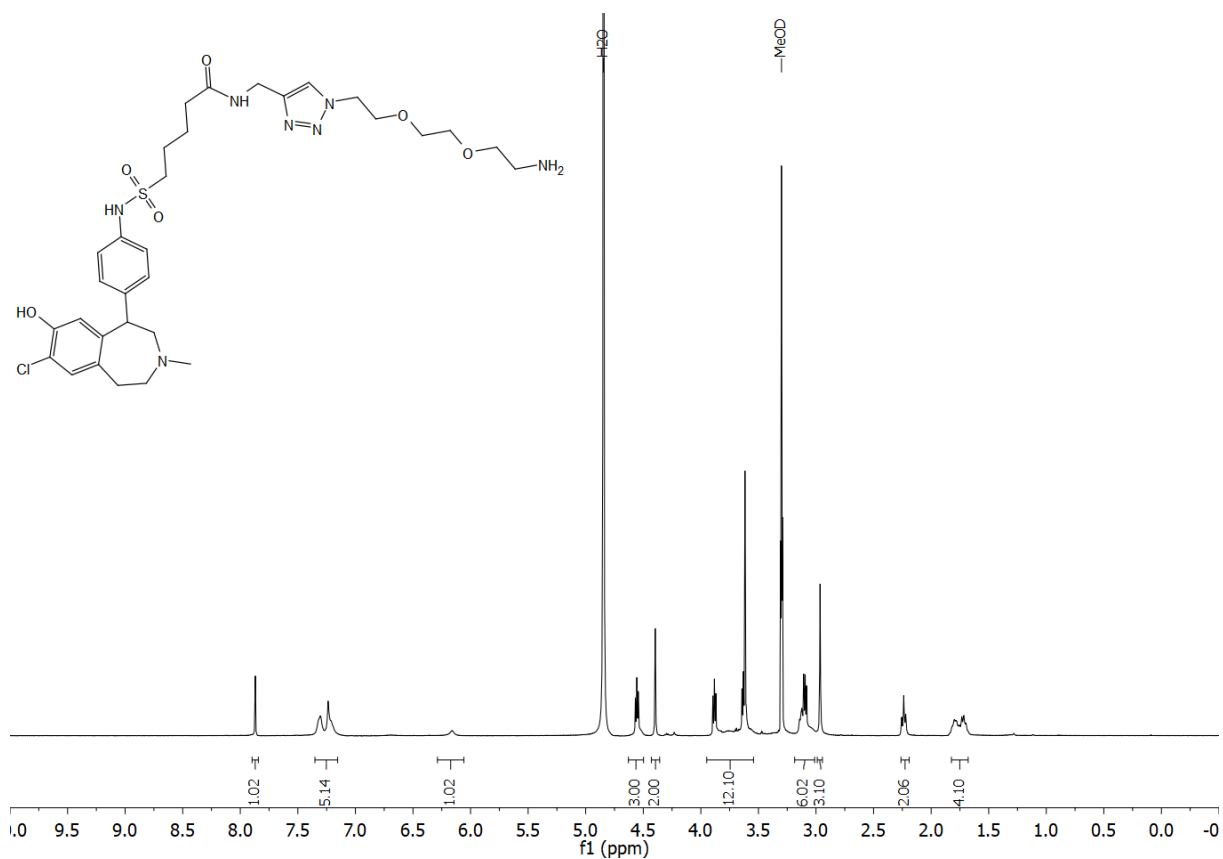**Figure S25.** ¹H NMR spectrum (400 MHz, MeOD) of compound **22b**.

5. Structures of the fluorescent ligands 23-28

Figure S26. Structure of compound **23**.

Figure S27. Structure of compound **24**.

Figure S28. Structure of compound **25**.
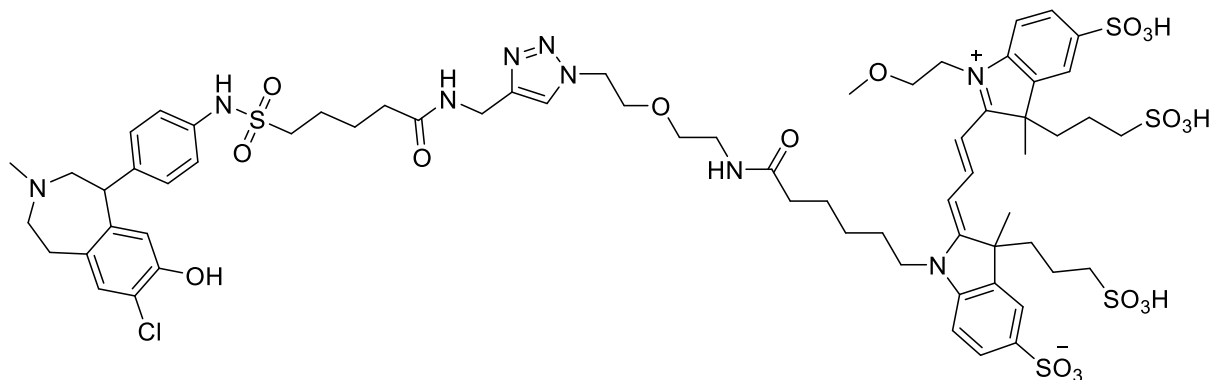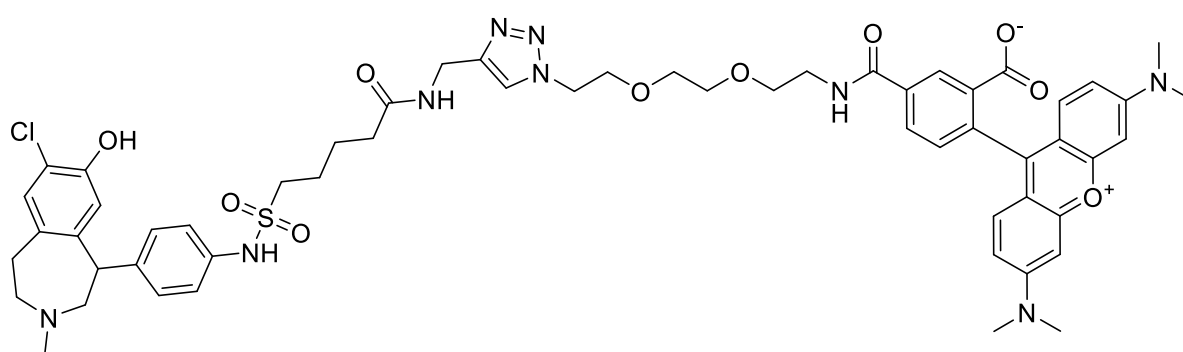
Figure S29. Structure of compound **26**.

Figure S30. Structure of compound **27**.

Figure S31. Structure of compound **28**.

6. Binding poses of SKF-83959 bound to the D$_1$R
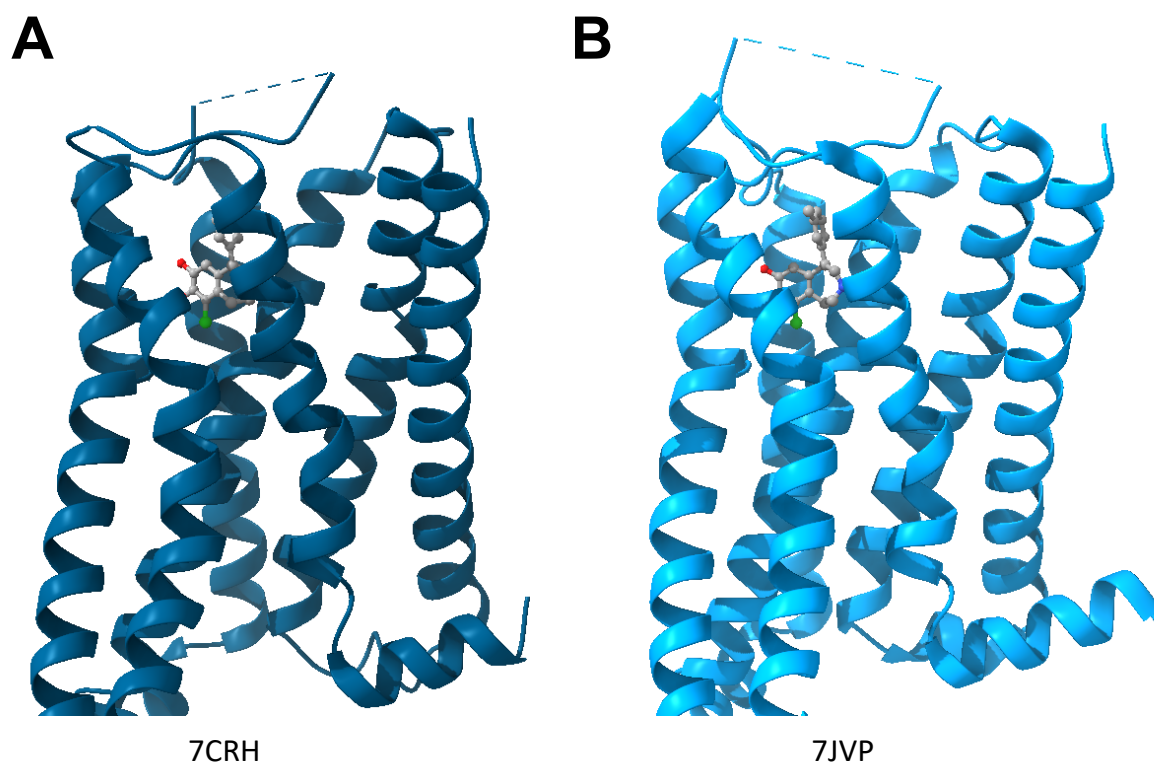
A

B

7CRH

7JVP

Figure S32. Binding poses of SKF-83959 bound to the D$_1$R in complex with Gs protein (Gs protein not depicted) based on the cryo-EM structures 7CRH[1] (**A**) and 7JVP[2] (**B**).

7. References

[1] P. Xiao, W. Yan, L. Gou, Y.-N. Zhong, L. Kong, C. Wu, X. Wen, Y. Yuan, S. Cao, C. Qu, X. Yang, C.-C. Yang, A. Xia, Z. Hu, Q. Zhang, Y.-H. He, D.-L. Zhang, C. Zhang, G.-H. Hou, H. Liu, L. Zhu, P. Fu, S. Yang, D. M. Rosenbaum, J.-P. Sun, Y. Du, L. Zhang, X. Yu, Z. Shao, *Cell* **2021**, *184*, 943-956.e18.

[2] Y. Zhuang, P. Xu, C. Mao, L. Wang, B. Krumm, X. E. Zhou, S. Huang, H. Liu, X. Cheng, X.-P. Huang, D.-D. Shen, T. Xu, Y.-F. Liu, Y. Wang, J. Guo, Y. Jiang, H. Jiang, K. Melcher, B. L. Roth, Y. Zhang, C. Zhang, H. E. Xu, *Cell* **2021**, *184*, 931-942.e18.